Journal of Materials Chemistry B

PAPER

View Article Online
View Journal



Cite this: DOI: 10.1039/c5tb00908a

# Electrodeposition of flower-like nickel oxide on CVD-grown graphene to develop an electrochemical non-enzymatic biosensor†

Arunkumar Rengaraj,‡[a] Yuvaraj Haldorai,‡[b] Cheol Hwan Kwak,[b] Seungbae Ahn,[c] Ki-Joon Jeon,[c] Seok Hoon Park,[d] Young-Kyu Han*[b] and Yun Suk Huh*[a]

Received 13th May 2015,
Accepted 26th June 2015

DOI: 10.1039/c5tb00908a

www.rsc.org/MaterialsB

We demonstrated a non-enzymatic cholesterol sensor based on a nickel oxide (NiO) and high quality graphene composite for the first time. Graphene was grown by a chemical vapor deposition technique (CVD). The nanocomposite was fabricated through the electrodeposition of nickel hydroxide onto the surface of the CVD-grown graphene, which was followed by thermal annealing. The successful formation of the NiO/graphene composite was confirmed by X-ray diffraction, X-ray photoelectron spectroscopy, and Raman spectroscopy. The deposition of flower-like NiO onto the graphene surface was confirmed by scanning electron microscopy. Electrochemical analyses were conducted to investigate the characteristics of the sensor during the detection of cholesterol. The sensor showed a high sensitivity of 40.6 mA $\mu M^{-1}$ $cm^{-2}$, a rapid response time of 5 s, and a low detection of limit of 0.13 μM. We also investigated the effects of common interfering substances on the ability of the sensor to detect cholesterol. Furthermore, we successfully determined the cholesterol in a milk sample using the developed sensor. The composite electrode exhibited excellent detection of cholesterol with good reproducibility and long-term stability owing to the combined effects of NiO and graphene.

## Introduction

Two-dimensional $sp^2$ carbon nanomaterial graphene has attracted increasing interest because of its unique physical and chemical properties, which include high surface area, good chemical resistance, excellent electrical conductivity, extraordinary mechanical properties, high charge mobility, and thermal conductivity.[1–4] Hence, graphene is ideal for use in fundamental research. Graphene is also an excellent support material for the preparation of multifunctional nanomaterials. For example, graphene has been used as an attractive building block during the preparation of various nanocomposites for use in extensive applications. In several recent applications, graphene has been combined with different nanomaterials including noble metals,[5,6] metal oxides,[7–9] metal sulfides,[10,11] and metal hydroxides.[12,13]

Transition metal oxides have attracted much attention in recent years because of their unique properties.[14–19] In particular, nickel oxide (NiO) has received a great deal of interest because of its wide bandgap, large specific capacitance, good electrochemical stability, and low cost. Accordingly, it has been used in a wide range of applications including supercapacitors, Li-ion batteries, and biosensors.[20–24] Nanostructured NiO materials have been used in enzyme-free glucose sensors because of their high electrocatalytic activity.[22–24] However, the poor electronic conductivity of NiO significantly affects its sensing properties. A common strategy used to enhance charge transport in electrochemical sensors is the combination of highly electrocatalytic materials with conductive substances such as conducting polymers, carbon nanotubes (CNTs), and graphene, which increase the conductivity of NiO.

Several studies have reported various approaches to the synthesis of NiO/graphene or CNT nanocomposites for use as electrochemical biosensors. For example, Shamsipur *et al.*[25] employed an electrochemical method to prepare a multi-walled carbon nanotube/NiO composite, which greatly improved the electrooxidation of glucose. Lv *et al.*[26] used a multi-step self-assembly approach to synthesize graphene nanosheet/NiO hybrid materials for use in an enzyme-free glucose sensor.

[a] Department of Biological Engineering, Biohybrid Systems Research Center (BSRC), Inha University, Incheon, 402-751, Republic of Korea. E-mail: yunsuk.huh@inha.ac.kr; Fax: +82-32-872-4046
[b] Department of Energy and Materials Engineering, Dongguk University-Seoul, Seoul 100-715, Republic of Korea. E-mail: ykenergy@dongguk.edu; Fax: +82-2-2268-8550
[c] Department of Environmental Engineering, Inha University, Incheon, 402-751, Republic of Korea
[d] Department of Enviromental Engineering, Anyang University, Anyang-si, 430-714, Republic of Korea

† Electronic supplementary information (ESI) available. See DOI: 10.1039/c5tb00908a

‡ These authors contributed equally to this work.

Yuan *et al.*[27] electrodeposited a graphene oxide/NiO composite on a glassy carbon electrode to develop a non-enzymatic glucose sensor. Zhu *et al.*[28] developed an amperometric non-enzymatic glucose sensor based on a NiO/reduced graphene oxide composite. Li *et al.*[29] recently demonstrated the facile one-step electrochemical synthesis of graphene/NiO composites for application in a glucose and methanol sensor. Sun *et al.*[30] reported an electrochemical DNA sensor based on a graphene/NiO composite modified carbon ionic liquid electrode. Although CNT- or graphene/NiO-based composites have been used for the detection of various biomolecules, few studies have investigated the electrochemical detection of cholesterol.

We report here a non-enzymatic electrochemical cholesterol sensor based on NiO/high quality graphene nanocomposites. To the best of our knowledge, this is the first such sensor to be developed. The nanocomposite was fabricated through electrodeposition, and high-quality graphene was synthesized by a chemical vapor deposition (CVD) method. There are different methods in which graphene monolayers can be synthesized. The most widespread method is by using a CVD technique. This method can be used to produce high quality graphene, potentially on a large scale. The as-synthesized nanocomposite was characterized by X-ray diffraction (XRD), Raman spectroscopy, scanning electron microscopy (SEM), and X-ray photoelectron spectroscopy (XPS). Electrochemical studies used to evaluate the electrocatalytic performance of the nanocomposite revealed excellent sensitivity of the detection of cholesterol because of the synergetic effects of NiO and CVD-grown graphene. In addition, the effects of common interfering materials on cholesterol sensing were investigated.

## Materials and methods

### Materials

Cholesterol, ascorbic acid, uracil, uric acid, Triton X-100, and nickel(II) nitrate hexahydrate ($Ni(NO_3)_2$) were purchased from Sigma Aldrich. All other reagents were of analytical grade and used as received. Unless otherwise specified, deionized water was used throughout this study.

### Synthesis of graphene by a chemical vapor deposition technique

Graphene was grown on 25 μm thick copper foil by a CVD technique using a mixture of methane and hydrogen. The copper foil was first annealed in hydrogen at ~1000 °C for 20 min. Graphene was then grown over methane and hydrogen at the same temperature for 10 min. A thin poly(methylmethacrylate) (PMMA) film was subsequently spin-coated on a graphene/copper substrate at 2000 rpm. After drying overnight at room temperature, the graphene on the backside of the Cu foil was removed by plasma etching for 2 min. The Cu was then dissolved in ammonium persulfate aqueous solution, after which it was washed with DI water. The floating graphene/PMMA was scooped onto the $SiO_2$/Si substrate (1 × 1 cm), dried under vacuum overnight and then baked at 150 °C for 10 min. Finally, PMMA was dissolved in acetone.

### Synthesis of the NiO/graphene nanocomposite

The one-step electrochemical synthesis of the NiO/graphene nanocomposite was carried out by scanning the potential of the graphene/GCE between −1.2 and 0 V *versus* SCE at a scan rate of 50 mV $s^{-1}$ for 30 cycles in 0.1 M acetate buffer solution (ABS, pH 4.0) containing 10 mM $Ni(NO_3)_2$ as an electrolyte. After deposition, the electrode was rinsed with distilled water and then annealed at 270 °C for 3 h in air.

### Preparation of the cholesterol sample

The cholesterol solution (5 mM) was prepared by dissolving 0.097 g of cholesterol in 50 mL of phosphate buffer (0.05 mM, pH 6.8) containing 1 mL of isopropanol and 5 mL of Triton X-100. The solution was heated at 60 °C for 1 h.

### Electrochemical analysis

The electrochemical performance was evaluated using a three-electrode cell system. Cyclic voltammetry (CV) and chronoamperometric experiments were conducted on a CHI 660D electrochemical workstation at room temperature. A 1 M KOH solution was used as an electrolyte, and the NiO/SLG nanocomposite was used as a working electrode. A platinum wire was employed as a counter electrode and Ag/AgCl as the reference. The chronoamperometric experiments were performed by stirring the solution at 600 rpm.

### Characterization

SEM images were recorded using a Hitachi S-4300 microscope equipped with an energy-dispersive X-ray detector (EDS), which was operated at an accelerating voltage of 20 kV. The Raman spectra of the samples were obtained using a HR800 UV Raman microscope (Horiba Jobin-Yvon, France). XRD patterns were collected using an X'Pert PRO MRD (Philips) diffractometer with Cu Kα radiation. XPS measurements were obtained using a Thermo Scientific, K-Alpha electron spectrometer with an Al X-ray source.

## Results and discussion

Fig. 1 shows a schematic diagram of the fabrication of the NiO/graphene nanocomposite. High quality graphene was synthesized by the CVD technique and transferred into the $SiO_2$/Si substrate, after which NiO was electrodeposited onto the graphene surface. The as-prepared NiO/graphene nanocomposite was used to investigate the enzyme-free electrochemical detection of cholesterol.

Raman spectroscopy is generally used to characterize carbonaceous materials. Fig. 2 shows the Raman spectra of graphene and the NiO/graphene nanocomposite. The CVD-grown graphene (Fig. 2a) exhibited three bands, D, G, and 2D, at 1334, 1591, and 2679 $cm^{-1}$, respectively. The D band represents the disordered carbon arising from structural defects,[31,32] while the

 

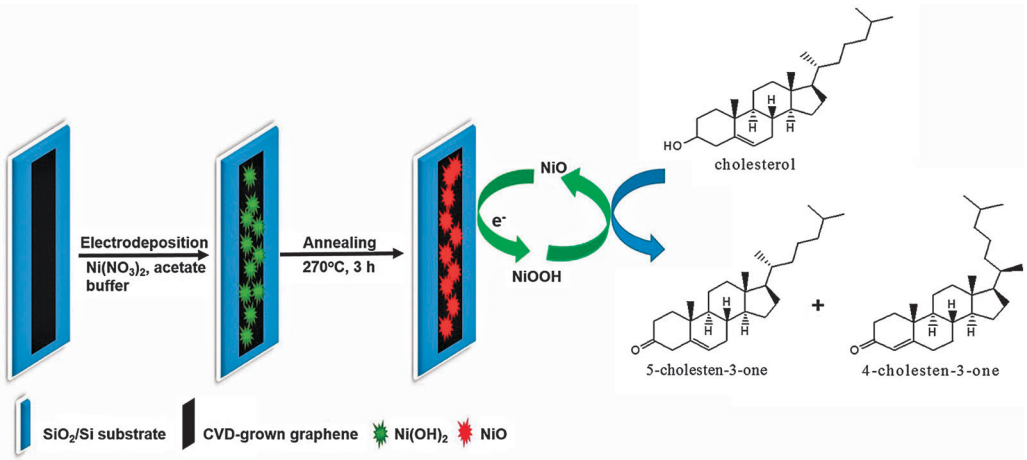


Fig. 1 Schematic diagram of the fabrication of the NiO/graphene composite electrode for cholesterol sensing.

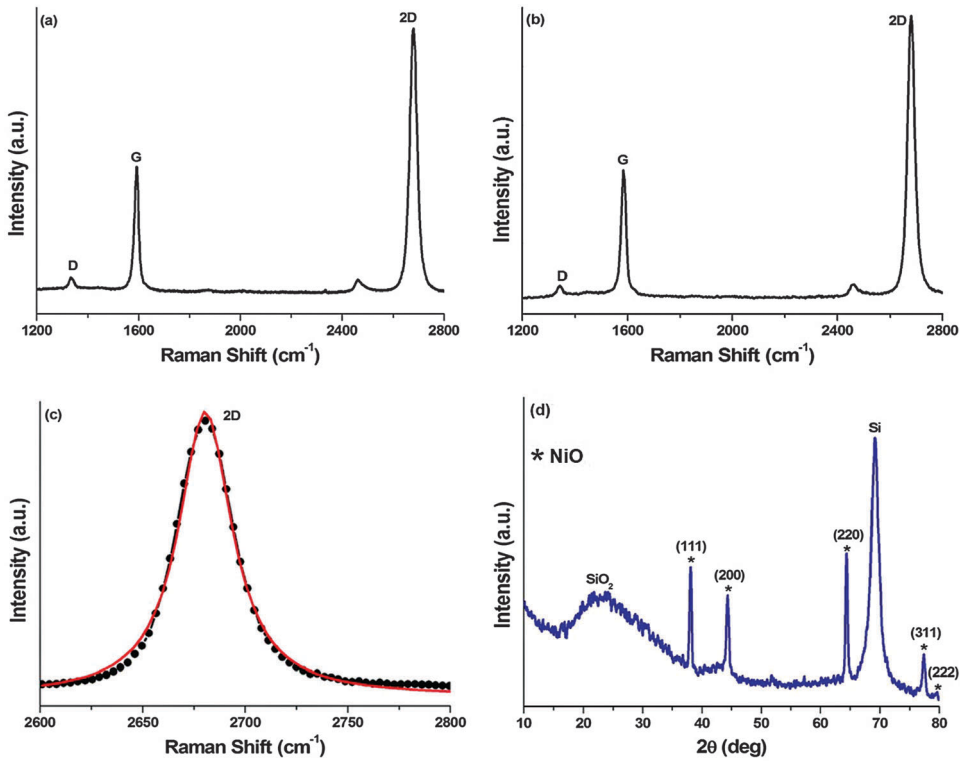


Fig. 2 Raman spectra of (a) graphene, (b) the NiO/graphene nanocomposite, (c) the 2D band of graphene fitting with a single Lorentzian peak centered at 2679 $cm^{-1}$, and (d) the XRD pattern of the nanocomposite.

G band corresponds to the $E_{2g}$ phonon of $sp^2$ carbon atoms. The extremely weak D band in the spectrum confirmed the high quality of the graphene sample, which had a few structural defects. In the nanocomposite (Fig. 2b), the aforementioned bands were shifted to 1341, 1588, and 2687 $cm^{-1}$, respectively, which was ascribed to the interaction between NiO and graphene.

Raman analysis was also employed to investigate the number of graphene layers present. According to the literature,[31–34] the shape and position of the G and 2D bands were correlated with the number of graphene layers.[31,32] Graphene synthesized by the CVD technique showed the full width of the sharp G band (1591 $cm^{-1}$) at half a maximum of 30 $cm^{-1}$ and a single Lorentzian profile of the 2D band (2679 $cm^{-1}$), which verified the SLG. Fig. 2c shows the peak fitting of the 2D band. The spectrum showed a single peak, which was identical to the SLG.[35] In addition, the 2D/G intensity ratio ($I_{2D}/I_G$) showed a good relationship with the number of graphene layers. The $I_{2D}/I_G$ ratios of single-layer, double-layer, and multi-layer graphene were $>2$, 1–2, and $<1$, respectively.[33,34] The $I_{2D}/I_G$ ratio of the as-synthesized graphene was calculated to be 2.1, which was

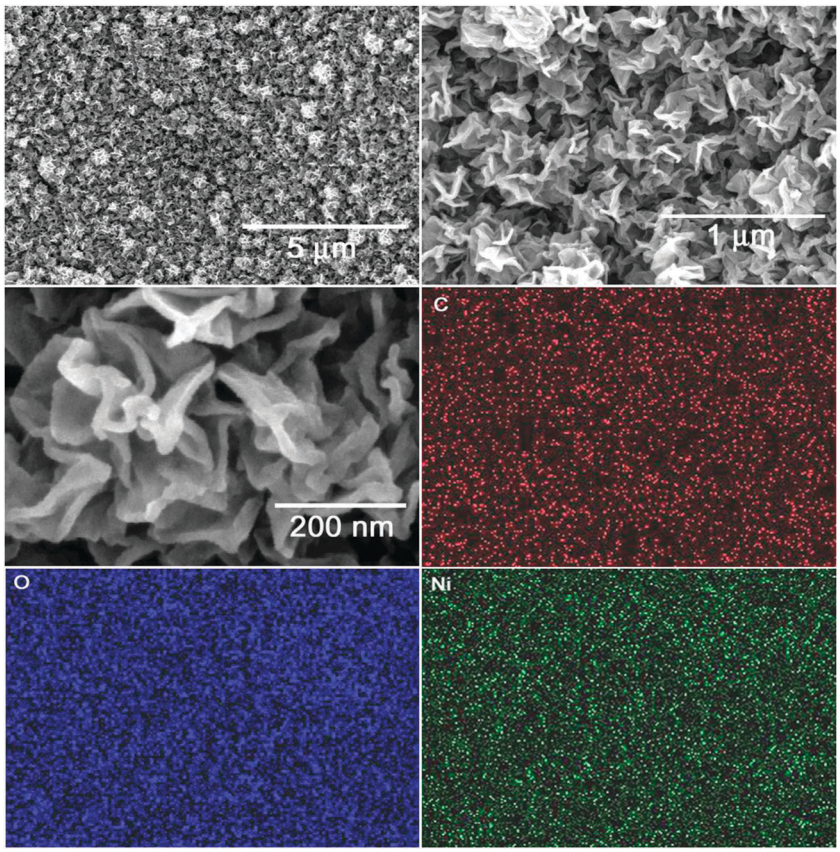


Fig. 3 SEM images (low & high resolution) and elemental mapping of the NiO/graphene nanocomposite.

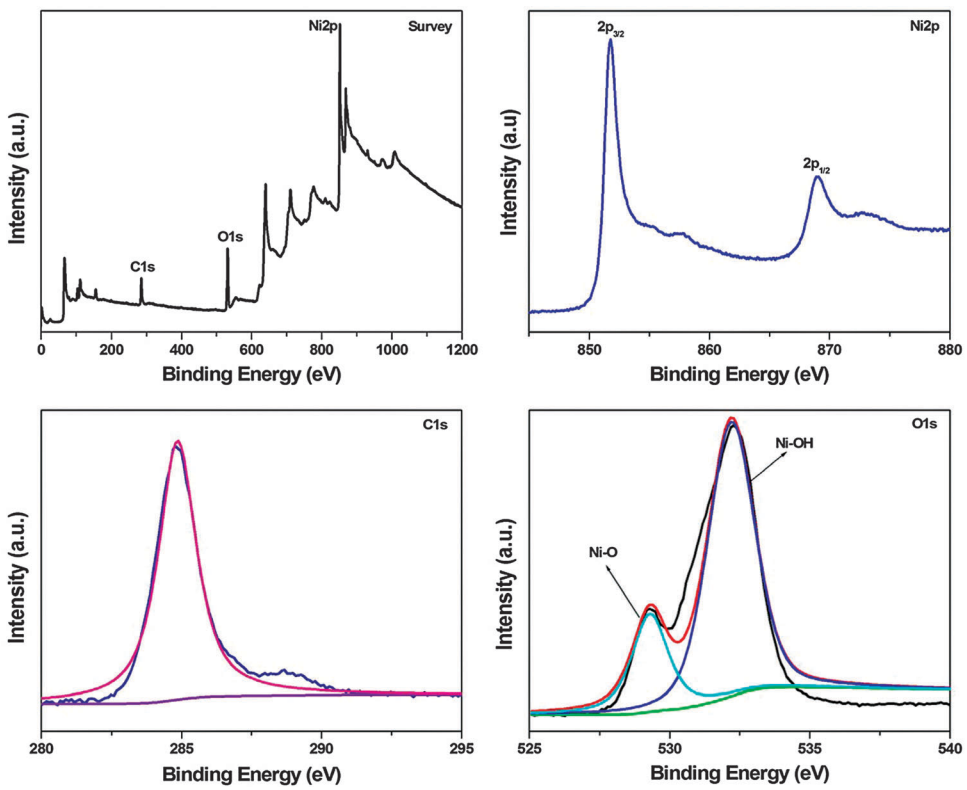


Fig. 4 Survey, N 2p, C 1s, and O 1s core-level spectra of the nanocomposite.

comparable to the CVD-grown monolayer graphene.[32] Therefore, the results showed that the as-grown graphene was a single layer.

XRD was used to examine the crystallinity and purity of the sample. Fig. 2d shows the XRD pattern of the as-synthesized NiO/graphene nanocomposite. Diffraction peaks were observed at $2\theta$ = 38.0°, 44.2°, 64.3°, 77.0°, and 79.5°, which were indexed to the (111), (200), (220), (311), and (222) reflections, respectively, of the face-centered cubic structure of NiO (JCPDS, No. 04-0835). The broad peak observed at 22.6° was indicative of the amorphous $SiO_2$ (from substrate), while the intense peak observed at 69.0° was assigned to the silicon substrate. XRD patterns of the as-grown graphene and the bare substrate ($SiO_2$/Si) are given in Fig. S1 as a reference (ESI†).

SEM and EDS analyses of the as-synthesized NiO/graphene nanocomposite are shown in Fig. 3. It can be seen from Fig. 3 that flower-like NiO nanostructures were densely coated onto the entire graphene surface. EDS mapping analysis indicated the existence of elements Ni, O (from NiO) and C (graphene) in the composite. The SEM images of the CVD-grown graphene are shown in Fig. S2 (ESI†).

Fig. 4 demonstrates the survey and core-level spectra of the NiO/graphene nanocomposite. The survey spectrum exhibited C 1s (285.0), O 1s (531.8), and Ni 2p (851.9 eV) peaks, which confirmed the successful formation of NiO onto the graphene surface. The core-level spectrum of Ni 2p has two peaks, a main peak ($2p_{3/2}$) and a satellite peak ($2p_{1/2}$), with binding energies of 851.9 eV and 868.5 eV, respectively. The peak positions were identical to the $2p_{3/2}$ and $2p_{1/2}$ peaks in NiO.[36,37] The Gaussian fit of the C 1s core-level spectrum showed a main peak at 284.3 eV, which corresponded to the $sp^2$ C–C bond. The O 1s spectrum was deconvoluted into two peaks, one at 529.3 eV attributed to the Ni–O bond, and another at 532.0 eV that was ascribed to a defective NiO with hydroxyl groups absorbed on its surface (Ni–OH). These results are consistent with the findings of previous studies.[38,39]

Fig. 5 shows the CV of graphene and the NiO/graphene nanocomposite at a scan rate of 100 mV $s^{-1}$ in 1 M KOH.

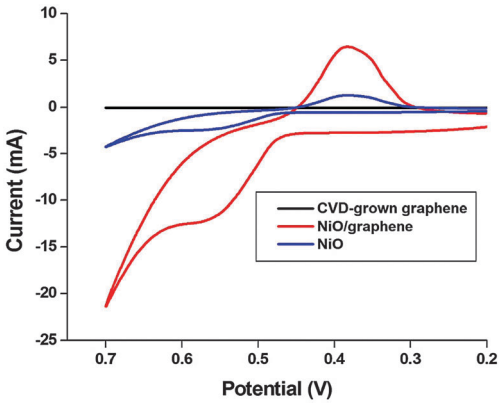


Fig. 5 CV of graphene, NiO, and the NiO/graphene nanocomposite in 1 M KOH solution at a scan rate of 100 mV $s^{-1}$.

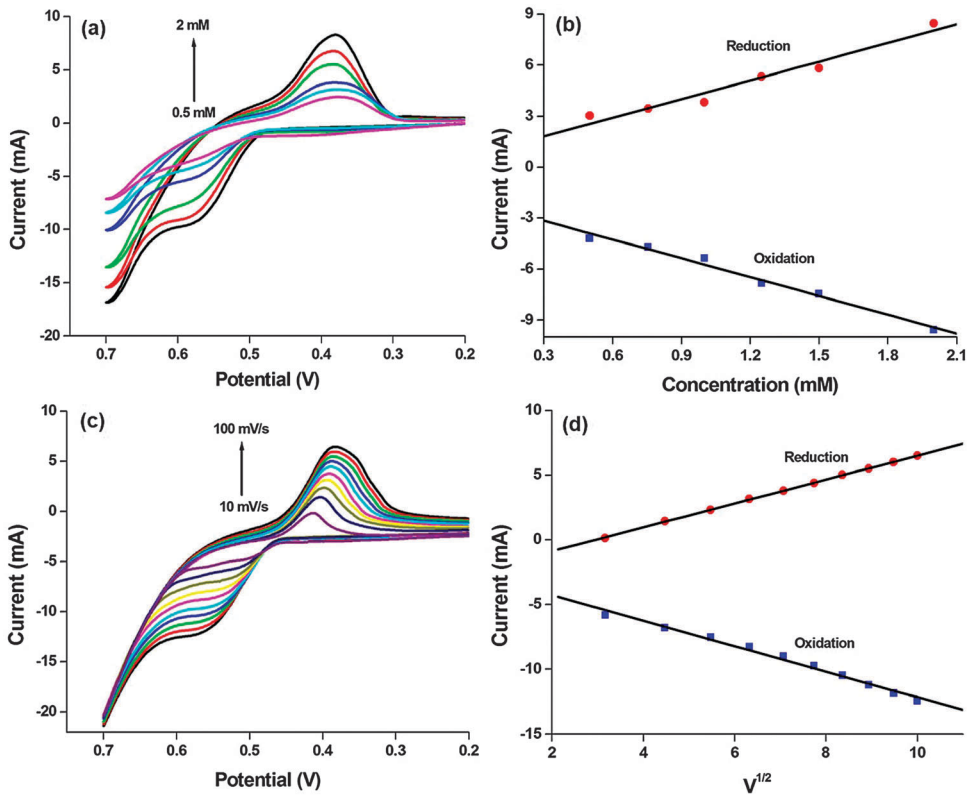


Fig. 6 (a) CV of the nanocomposite in 1 M KOH at different cholesterol concentrations (scan rate = 100 mV $s^{-1}$), (b) the plot of peak current *versus* concentration, (c) CV of the nanocomposite at different scan rates in 1 M KOH, and (d) the plot of peak current *versus* square root of the scan rate.

Graphene showed no redox peaks in the given potential range of 0.2 to 0.7 V, whereas the nanocomposite exhibited anodic and cathodic peaks at around 0.58 V and 0.39 V, respectively. These results can be ascribed to the synergic effect of NiO and graphene. The high electrocatalytic activity of NiO and the large active surface area and better conductivity of graphene resulted in the increased current of the nanocomposite, which is concordant with the findings of previous studies[40,41] of the electrochemical reaction of NiO in alkaline solution. As a reference, the CV of pure NiO was also given. The mechanism involved hydroxyl ions ($OH^-$) in the redox reactions of NiO. As shown in Fig. 5, the redox peaks were ascribed to the transition between NiO and NiOOH. The reaction is expressed by eqn (1).[26–28]

$$NiO + OH^- \leftrightarrow NiOOH + e^- \quad (1)$$

Fig. 6a illustrates the CV of the NiO/graphene nanocomposite with different cholesterol concentrations at a scan rate of 100 mV $s^{-1}$ in 1 M KOH. The current of the oxidation peak increased linearly according to the cholesterol concentration, which indicated that the nanocomposite electrode had excellent sensitivity to cholesterol. A positive shift in the redox peaks could be attributed to the adsorption of cholesterol, as well as the oxidized products of cholesterol on the composite surface, which may control the kinetics of the electrochemical reactions.[42] The mechanism of cholesterol electrooxidation in the NiO/graphene nanocomposite electrode is explained by the following equations. In the first step, NiO was electrochemically oxidized to NiOOH in basic solution (eqn (1)), where an electron was released. In the second step, cholesterol was oxidized to cholestenone[43] by NiOOH, which was simultaneously reduced to NiO. The reaction is represented by eqn (2):

$$Ni^{3+} + \text{cholesterol} \rightarrow Ni^{2+} + \text{cholestenone} \quad (2)$$

Fig. 6b shows a typical graph of the peak current *versus* cholesterol concentration. The anodic and cathodic peak current gradually increased as the cholesterol concentration increased (0.5 mM to 2 mM). The regression coefficient ($R^2$) values of 0.992 ($I_{pa}$) and 0.999 ($I_{pc}$) indicated the excellent detection of cholesterol.

Fig. 6c demonstrates the CV of the NiO/graphene nanocomposite at different scan rates in the presence of 0.5 mM cholesterol in 1 M KOH. The anodic and cathodic peak current increased significantly when the scan rate increased from 10 to 100 mV $s^{-1}$, showing a linear relationship with the square root of the scan rate with $R^2$ values of 0.994 ($I_{pa}$) and 0.978 ($I_{pc}$) (Fig. 6d). These results suggested that the electrochemical reaction was confined to the surface.

Fig. 7a shows the amperometric response of the NiO/graphene nanocomposite electrode to successive step-wise additions of cholesterol to 1 M KOH. A significant increase in peak current was observed when cholesterol was added to the stirred KOH solution. The electrode exhibited a rapid response

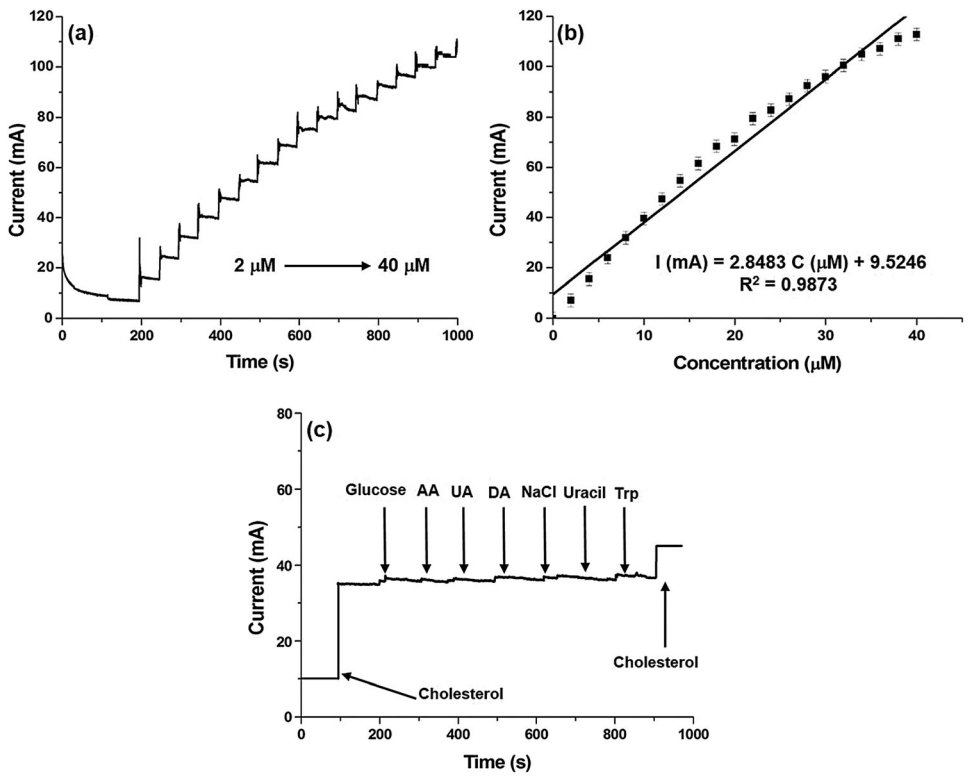


Fig. 7 (a) Chronoamperometric data of the nanocomposite electrode toward successive addition of cholesterol in 1 M KOH, (b) the plot of peak current *versus* concentration, and (c) the interference test of the nanocomposite electrode in 1 M KOH with 20 μM cholesterol in the presence of 20 μM glucose, 20 μM AA, 20 μM UA, 20 μM DA, 40 μM NaCl, 40 μM uracil, and 20 μM Trp.

 

Table 1 Comparison of the results of the present study with previous reports for cholesterol sensing

| Electrode | Detection limit | Linear range | Sensitivity |
|---|---|---|---|
| MWCNT@MIP–CCE[44] | 1 nM | 10–300 nM | — |
| AuNPs–MWCNTs/GCE[45] | $3.3 \times 10^{-14}$ mol $L^{-1}$ | $1 \times 10^{13}$–$1 \times 10^{9}$ mol $L^{-1}$ | — |
| ChOx/chitosan–ZnO/ITO[46] | 5 mg $dl^{-1}$ | 5–300 mg $dl^{-1}$ | $1.41 \times 10^{-4}$ A mg $dl^{-1}$ |
| ChOx/PANI–MWCNT/ITO[47] | — | 1.29–12.93 mM | 6800 nA $mM^{-1}$ |
| ChOx/$CeO_2$/graphene/GCE[48] | 4.0 μM | 12 μM–7.2 mM | — |
| Graphene/β-CD[43] | 1 μM | 0.005–0.03 mM | 0.01 μA $\mu M^{-1}$ |
| ChOx/NiO–chitosan/ITO[49] | 43.4 mg $dl^{-1}$ | 10–400 mg $dl^{-1}$ | 0.808 μA $mg^{-1}$ $dl^{-1}$ $cm^{-2}$ |
| NiO nanorods[50] | 0.65 mM | 0.64–10.3 mM | 120 mA $mM^{-1}$ |
| NiO/CVD-grown graphene (present work) | 0.13 μM | 2–40 μM | 40.6 mA $\mu M^{-1}$ $cm^{-2}$ |

MWCNT – multi-walled carbon nanotube; MIP – molecular imprinted polymer; CCE – ceramic carbon electrode; GCE – glassy carbon electrode; PANI – polyaniline; CD – cyclodextrin.

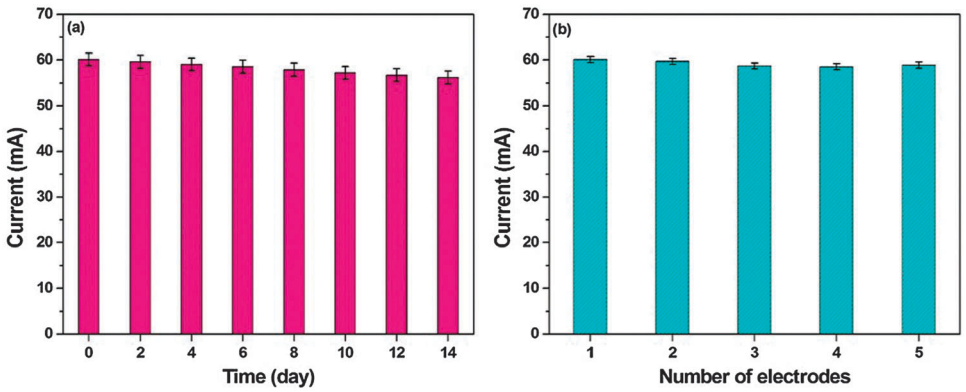


Fig. 8 (a) Amperometric response *versus* time for the oxidation of cholesterol at the electrode in 1 M KOH demonstrating the operational stability of the electrode and (b) peak current at five different composite electrodes for the detection of 20 μM cholesterol showing good reproducibility.

to the cholesterol, reaching a plateau within 5 s. Fig. 7b shows the calibration curve for the measurement of the cholesterol. The electrode showed a linear relationship with the cholesterol concentration (2–40 μM) using a regression equation of $I$ (mA) = 2.8483 $C$ (μM) + 9.5264 ($R^2$ = 0.9873). The low detection limit of cholesterol sensing was identified at 0.13 μM. Taken together, these results indicated that the composite electrode had excellent ability for non-enzymatic detection of cholesterol. The linear range, detection limit, and sensitivity of other electrodes are compared to those of the NiO/graphene nanocomposite electrode and listed in Table 1. Even though previously reported enzymatic and non-enzymatic cholesterol sensors based on other nanomaterials showed good performance,[43–50] the performance of the NiO/graphene composite may be attributed to the large surface area of the nanocomposite and good electron transfer between NiO and graphene. Because of the high surface area, the composite can adsorb and catalyze more reactive substances, resulting in an instantaneous oxidation process.

Selectivity is an important parameter of the non-enzymatic cholesterol sensor. It is well known that ascorbic acid (AA), uric acid (UA), uracil, glucose, tryptophan (Trp), dopamine (DA) and sodium chloride (NaCl) interfere with the detection of cholesterol. Therefore, in this study, glucose (20 μM), AA (20 μM), UA (20 μM), DA (20 μM), NaCl (40 μM), uracil (40 μM), and Trp (20 μM) were added at selected concentrations to mimic the interference. As shown in Fig. 7c, these materials had no significant effects on the cholesterol sensing ability of the electrode at the tested concentrations.

Table 2 Determination of cholesterol in milk samples ($n$ = 4)

| Sample | Diluted sample (mM) | Spiked (mM) | Detected (mM) | RSD (%) | Recovery (%) |
|---|---|---|---|---|---|
| 1 | 0.2 | 0.5 | 0.67 | 2.14 | 95.7 |
| 2 | 0.13 | 0.3 | 0.42 | 1.32 | 97.7 |
| 3 | 0.08 | 0.2 | 0.275 | 1.87 | 98.2 |
| 4 | 0.05 | 0.15 | 0.204 | 1.19 | 102 |

The shelf-life of the nanocomposite electrode was checked after two weeks (Fig. 8a). To accomplish this, the electrode was stored in a vacuum at room temperature (24 °C), during which the detection of 20 μM cholesterol was monitored at regular two day intervals. The high stability of the electrode may be attributed to the good chemical stability of NiO in the electrolyte. We also demonstrated the reproducibility of sensor fabrication by measuring the changes in peak current of five NiO/graphene nanocomposite electrodes during cholesterol detection. As shown in Fig. 8b, the sensor exhibited good reproducibility.

To validate the feasibility of the fabricated cholesterol sensor, the amount of cholesterol in milk samples was determined. Specifically, four milk samples of different concentrations (0.2, 0.13, 0.08, and 0.05 mM) were prepared by diluting samples of known cholesterol concentration in 1 M KOH. The results

summarized in Table 2 indicated that the sensor showed excellent detection of cholesterol in milk samples.

## Conclusions

We successfully fabricated a NiO/graphene nanocomposite by electrodeposition of NiO onto the surface of CVD-grown graphene, which was then used to investigate the non-enzymatic detection of cholesterol. The SEM analysis showed that flower-like NiO was densely decorated onto the graphene surface. The composite electrode detected a range of cholesterol concentrations from 2 μM to 40 μM with high sensitivity. Additionally, a low detection limit and a rapid response time of 0.13 μM and 5 s, respectively, were observed. Moreover, interference materials (AA, UA, uracil, glucose, Trp, DA, and NaCl) exerted no significant effects on the detection of cholesterol. The high sensitivity of cholesterol could be attributed to the excellent electrocatalytic activity of NiO and the large specific surface area of graphene. In addition, the high stability and shelf-life make this composite electrode a suitable device for the detection of cholesterol in biological samples. This synthetic procedure could be extended to the preparation of a wide range of graphene/metal oxide nanocomposites for energy and environmental applications.

## Acknowledgements

This work was supported by a National Research Foundation of Korea (NRF) grant funded by the Korean Ministry of Science, ICT & Future Planning (2010-C1AAA001-0029018) and the Basic Science Research Program through the National Research Foundation of Korea (NRF) funded by the Ministry of Science, ICT & Future Planning (No. 2014R1A5A1009799) and (NRF-2014R1A2A1A11053567). This work was also supported by the Dongguk University Research Fund of 2013 and Inha University.

## Notes and references

1 K. S. Novoselov, A. K. Geim, S. V. Morozov, D. Jiang, M. I. Katsnelson, I. V. Grigorieva, S. V. Dubonos and A. Firsov, *Nature*, 2005, **438**, 197.
2 C. Berger, Z. Song, T. Li, X. Li, A. Y. Ogbazghi, R. Feng, Z. Dai, A. N. Marchenkov, E. H. Conrad, P. N. First and W. A. de Heer, *J. Phys. Chem. B*, 2004, **108**, 19912.
3 A. K. Geim and K. S. Novoselov, *Nat. Mater.*, 2007, **6**, 183.
4 A. Reina, X. T. Jia, J. Ho, D. Nezich, H. B. Son, V. Bulovic, M. S. Dresselhaus and J. Kong, *Nano Lett.*, 2009, **9**, 30.
5 M. G. Chung, D.-H. Kim, D. K. Seo, T. Kim, H. U. Im, H. M. Lee, J.-B. Yoo, S.-H. Hong and T. J. Kang, *Sen. Actuators B, Chem.*, 2012, **169**, 387.
6 Y. Lv, Y. Fang, Z. Wu, X. Qian, Y. Song, R. Che, A. M. Asiri, Y. Xia, B. Tu and D. Zhao, *Small*, 2014, **11**, 1003.
7 Y. Haldorai, W. Voit and J.-J. Shim, *Electrochim. Acta*, 2014, **120**, 65.
8 Y. Haldorai, A. Rengaraj, C. H. Kwak, Y. S. Huh and Y.-K. Han, *Synth. Met.*, 2014, **198**, 10.
9 B. G. Choi, M. H. Yang, W. H. Hong, J. W. Choi and Y. S. Huh, *ACS Nano*, 2012, **5**, 4020.
10 L. David, R. Bhandavat and G. Singh, *ACS Nano*, 2014, **8**, 1759.
11 X. Fu, T. Jiang, Q. Zhao and H. Yin, *J. Mater. Sci.*, 2012, **47**, 1026.
12 L. Zhang, Z. Xiong and X. S. Zhao, *J. Power Sources*, 2013, **222**, 326.
13 C.-C. Hu, J.-C. Chen and K.-H. Chang, *J. Power Sources*, 2013, **222**, 128–133.
14 K. Thangavelu, K. Parameswari, K. Kuppusamy and Y. Haldorai, *Mater. Lett.*, 2011, **65**, 1482.
15 Y. Haldorai, S. Chitra and J.-J. Shim, *Adv. Sci., Eng. Med.*, 2013, **5**, 1044.
16 Y. Haldorai and J.-J. Shim, *Mater. Lett.*, 2014, **116**, 5.
17 Y. Ding, Y. Wang, L. Su, M. Bellagamba, H. Zhang and Y. Lei, *Biosens. Bioelectron.*, 2010, **26**, 542.
18 J. Huang, L. Wang, C. Gu and J.-J. Shim, *Mater. Lett.*, 2014, **136**, 371.
19 J. Wu, Q. Wang, A. Umar, S. Sun, L. Huang, J. Wang and Y. Gao, *New J. Chem.*, 2014, **38**, 4420.
20 S. Ding, T. Zhu, J. S. Chen, Z. Wang, C. Yuan and X. W. Lou, *J. Mater. Chem.*, 2011, **21**, 6602.
21 T. Kavitha and H. Yuvaraj, *J. Mater. Chem.*, 2011, **21**, 15686.
22 S. Liu, B. Yu and T. Zhang, *Electrochim. Acta*, 2013, **102**, 104.
23 C. Guo, Y. Wang, Y. Zhao and C. Xu, *Anal. Methods*, 2013, **5**, 1644.
24 Z. H. Ibupoto, K. Khun, V. Beni and M. Willander, *Soft Nanosci. Lett.*, 2013, **3**, 46.
25 M. Shamsipur, M. Najafi and M. M. Hosseini, *Bioelectrochemistry*, 2010, **77**, 120.
26 W. Lv, F.-M. Jin, Q. Guo, Q.-H. Yang and F. Kang, *Electrochim. Acta*, 2012, **73**, 129.
27 B. Yuan, C. Xu, D. Deng, Y. Xing, L. Liu, H. Pang and D. Zhang, *Electrochim. Acta*, 2013, **88**, 708.
28 X. Zhu, Q. Jiao, C. Zhang, X. Zuo, X. Xiao, Y. Liang and J. Nan, *Microchim. Acta*, 2013, **180**, 477.
29 S.-J. Li, N. Xia, X.-L. Lv, M.-M. Zhao, B.-Q. Yuan and H. Pang, *Sens. Actuators B, Chem.*, 2014, **190**, 809.
30 W. Sun, X. Wang, Y. Lu, S. Gong, X. Qi, B. Lei, Z. Sun and G. Li, *Mater. Sci. Eng., C*, 2015, **49**, 34.
31 A. C. Ferrari, J. C. Meyer, V. Scardaci, C. Casiraghi, M. Lazzeri, F. Mauri, S. Piscanec, D. Jiang, K. S. Novoselov, S. Roth and A. K. Geim, *Phys. Rev. Lett.*, 2006, **97**, 187401.
32 A. Reina, X. Jia, J. Ho, D. Nezich, H. Son, V. Bulovic, M. S. Dresselhaus and J. Kong, *Nano Lett.*, 2009, **9**, 30.
33 H. Medina, Y.-C. Lin, C. Jin, C.-C. Lu, C.-H. Yeh, K.-P. Huang, K. Suenaga, J. Robertson and P.-W. Chiu, *Adv. Funct. Mater.*, 2012, **22**, 2123.
34 C. Shan, H. Tang, T. Wong, L. He and S.-T. Lee, *Adv. Mater.*, 2012, **24**, 2491.
35 Y. Hernandez, V. Nicolosi, M. Lotya, F. M. Blighe, Z. Y. Sun, S. De, I. T. McGovern, B. Holland, M. Byrne, Y. K. Gun'ko, J. J. Boland, P. Niraj, G. Duesberg, S. Krishnamurthy,

 

R. Goodhue, J. Hutchison, V. Scardaci, A. C. Ferrari and J. N. Coleman, *Nat. Nanotechnol.*, 2008, **3**, 563.
36 B. Varghese, M. V. Reddy, Z. Yanwu, C. S. Lit, T. C. Hoong, G. V. S. Rao, B. V. R. Chowdari, A. T. S Wee, C. T. Lim and C. H. Sow, *Chem. Mater.*, 2008, **20**, 3360.
37 L. Liu, Y. Li, S. M. Yuan, M. Ge, M. M. Ren, C. S. Sun and Z. Zhou, *J. Phys. Chem. C*, 2010, **114**, 251.
38 G. Zhou, D.-W. Wang, L.-C. Yin, N. Li, F. Li and H.-M. Cheng, *ACS Nano*, 2012, **6**, 3214.
39 W. Liu, C. Lu, X. Wang, K. Liang and B. K. Tay, *J. Mater. Chem. A*, 2015, **3**, 624.
40 K. C. Liu and M. A. Anderson, *J. Electrochem. Soc.*, 1996, **143**, 124.
41 C. Natarajan, H. Matsumoto and G. Nogami, *J. Electrochem. Soc.*, 1997, **144**, 121.
42 P. Lu, J. Yu, Y. Lei, S. Lu, C. Wang, D. Liu and Q. Guo, *Sens. Actuators B, Chem.*, 2015, **208**, 90.
43 N. Agnihotri, A. D. Chowdhury and A. De, *Biosens. Bioelectron.*, 2015, **63**, 212.
44 Y. Tong, H. Li, H. Guan, J. Zhao, S. Majeed, S. Anjum, F. Liang and G. Xu, *Biosens. Bioelectron.*, 2013, **47**, 553.
45 J. Ji, Z. Zhou, X. Zhao, J. Sun and X. Sun, *Biosens. Bioelectron.*, 2015, **66**, 590.
46 R. Khan, A. Kaushik, P. R. Solanki, A. A. Ansari, M. K. Pandey and B. D. Malhotra, *Anal. Chim. Acta*, 2008, **616**, 207.
47 C. Dhand, S. K. Arya, M. Datta and B. D. Malhotra, *Anal. Biochem.*, 2008, **383**, 194.
48 M. Zhang, R. Yuan, Y. Chai, C. Wang and X. Wu, *Anal. Biochem.*, 2013, **436**, 69.
49 J. Singh, P. Kalita, M. K. Singh and B. D. Malhotra, *Appl. Phys. Lett.*, 2011, **98**, 123702.
50 Md. A. Ali, P. R. Solanki, M. K. Patel, H. Dhayani, V. V. Agrawal, R. John and B. D. Malhotra, *Nanoscale*, 2013, **5**, 2883.